

# Observation of Forbidden Magnetic Dipole Transitions Emitted from Highly Charged Argon in LHD Discharges

KATAI Ryuji, MORITA Shigeru<sup>1</sup> and GOTO Motoshi<sup>1</sup>

*Department of Fusion Science, School of Physical Science, Graduate University for Advanced Studies, Toki 509-5292, Japan*

<sup>1</sup> *National Institute for Fusion Science, Toki 509-5292, Japan*

(Received: 4 October 2004 / Accepted: 28 April 2005)

## Abstract

Vacuum ultraviolet (VUV) and visible spectra have been measured using a 3 m normal incidence and two 50 cm Czerny-Turner spectrometers with CCD detectors, respectively, in order to observe forbidden magnetic dipole (M1) transitions in  $2s^22p^x$  ( $x = 1$  to 5) ground and  $2s2p$  excited configurations of highly charged argon produced in argon discharges of Large Helical Device (LHD). One of observed VUV lines was precisely identified as an M1 transition of Ar XII ( $2s^22p3^4S_{3/2} - ^2P_{3/2} : 649.03 \pm 0.02 \text{ \AA}$ ) by analyzing Doppler broadening. Four M1 transitions of Ar X ( $2s^22p^5^2P_{3/2} - ^2P_{1/2} : 5533 \text{ \AA}$ ), Ar XI ( $2s^22p^4^3P_2 - ^3P_1 : 6917 \text{ \AA}$ ), Ar XIV ( $2s^22p^2P_{1/2} - ^2P_{3/2} : 4413 \text{ \AA}$ ) and Ar XV ( $2s2p^3P_1 - ^3P_2 : 5944 \text{ \AA}$ ) have been observed in the visible spectral region. Temporal behaviors of the VUV and visible lines were examined for reliable identification, and a clear difference was confirmed in comparison with those of Ar lines in lower-ionized stages. Wavelengths of the obtained M1 transitions were determined with high accuracy and compared with previous experimental and calculated values.

## Keywords:

vacuum ultraviolet, forbidden line, magnetic dipole transition, Doppler broadening, highly charged argon

## 1. Introduction

Forbidden lines arising from M1 transitions of highly charged ions are useful in plasma diagnostic applications because their long wavelengths compared with allowed transitions enable to observe Doppler broadening for ion temperature,  $T_i$ , and Doppler shift for plasma rotation. The M1 transitions of several highly charged ions have been studied in many laboratory and space plasmas, *e.g.*, Ti, Cr, Fe, Ni, Cu and Ge in PLT (Princeton Large Torus) [1-3], Ti in PDX (Poloidal Divertor Experiment) [4], Ti, Cr, Fe, Co and Ni in DITE (Divertor Injection Tokamak Experiment) [5], Ti, V, Cr, Fe, and Ni in TFR (Tokamak de Fontenay-aux-Roses) [6], Cu, Zn, Ga, As, Kr and Y in TEXT (Texas Experimental Tokamak) [7], Ti in ATF (Advanced Toroidal Facility) [8], Ni, Ge, Kr, Zr and Mo in JET (Joint European Torus) [9] and Fe in coronal plasmas using Hubble Space Telescope [10]. However, no reports on argon M1 transitions in VUV spectral region have been made in the field of high-temperature plasmas [11].

The M1 transitions in  $2s^22p^x$  ( $x = 1$  to 5) ground and  $2s2p$  excited configurations of highly charged argon have been identified using electron beam ion trap (EBIT) in visible spectral region [12,13], but the study of those transitions in VUV spectral region has not been

done so far.

Observation of the M1 transitions is generally difficult, because the M1 transitions are much weaker than allowed transitions. Argon is often used as radiation media for heat reduction in the divertor region of tokamaks [14]. In LHD, pure argon discharges have been carried out for ion heating experiments. In such discharges visible and VUV emissions from Ar ions drastically increased and the M1 transitions were observed for the first time in LHD. The central electron temperature is very high (4 keV) in the argon discharges. The M1 transitions of argon are emitted from the edge plasma due to a relatively small ionization potential of  $2s^22p^x$ ,  $2s2p$  configurations, although x-ray lines from H- and He-like argon are measured as a probe of core plasma ion temperature [15]. In this paper, the first observation of the Ar M1 transition in LHD is reported and results of the analysis are discussed.

## 2. Experimental setup

Argon discharges were produced by neutral beam heating with injection power up to 12 MW. The discharges were done at a standard configuration of LHD

under a magnetic field strength of 2.75 T and a magnetic axis of 3.60 m. The density was built up by Ar gas puff at the beginning of the discharge and maintained during 2 – 3 s with electron densities up to  $2 \times 10^{19} \text{ m}^{-3}$ . Almost pure argon discharges were performed remaining a small amount of hydrogen.

Vacuum ultraviolet (VUV) spectra have been measured using a space-resolved VUV system, consisting of a 3 m normal incidence spectrometer with a 1200 grooves/mm grating and with a reciprocal linear dispersion of  $2.75 \text{ \AA/mm}$ , CCD detector ( $1024 \times 1024$  pixels,  $13 \mu\text{m} \times 13 \mu\text{m}/\text{pixel}$ ) and a pair of two focusing mirrors [16]. Since emissions of the M1 transitions are essentially weak, a pair of two mirrors for radial profile measurement equipped in front of an incident slit of the spectrometer was removed and VUV emissions were directly measured to make the system brighter. A space-resolved slit set between the entrance slit and the grating was fully opened.

Visible spectra have been measured using two 50 cm Czerny-Turner type spectrometers equipped with CCD detectors ( $1024 \times 256$  pixels,  $26 \mu\text{m} \times 26 \mu\text{m}/\text{pixel}$ ). Low-resolution 100 and 150 grooves/mm gratings were selected for monitoring a wider spectral band. The plasma visible light was collected by a focusing lens set at a diagnostic port of LHD and transmitted by optical fibers with a core diameter of  $100 \mu\text{m}$ . Another side end of the fibers was coupled on the incident slit of the spectrometers. The CCD detectors were cooled down to  $-20^\circ \text{C}$  to decrease a thermal noise. As a result, the thermal noise count of the CCD detectors became smaller than 1 count/pixel. The CCD detectors were operated in 'full-binning mode', which means a full summation of vertical pixels, in order to take a better time resolution. The exposure time per a frame of the CCD detector was set to 50 ms.

### 3. Experimental results and discussion

The M1 transition of Ar XII ( $2s^2 2p^3 \ ^4S_{3/2} - \ ^2P_{3/2}$  :  $649.03 \text{ \AA}$ ) was identified in the VUV spectrum, as shown in Fig. 1. Most of the lines are also identified as indicated in the figure, although two Ar unclassified lines and five unknown lines are remained. The unknown lines have a narrow line width, and then should be arisen from lower ionization stages. The energy level diagram in  $2s^2 2p^3$  ground configuration of the Ar XII transitions is illustrated in Fig. 2 with their wavelengths calculated by the multi-configuration Dirac-Fock method [11]. The Ar XII M1 transitions are emitted in the VUV or microwave region. The arrow widths express relative amplitudes of calculated transition rates [11]. The observed Ar XII M1 transition

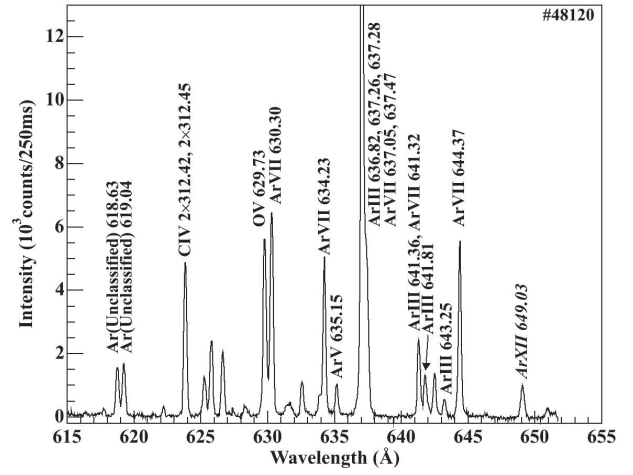


Fig. 1 VUV spectrum obtained from argon plasmas using 3 m normal incidence spectrometer. Italic fonts indicate Ar M1 line.

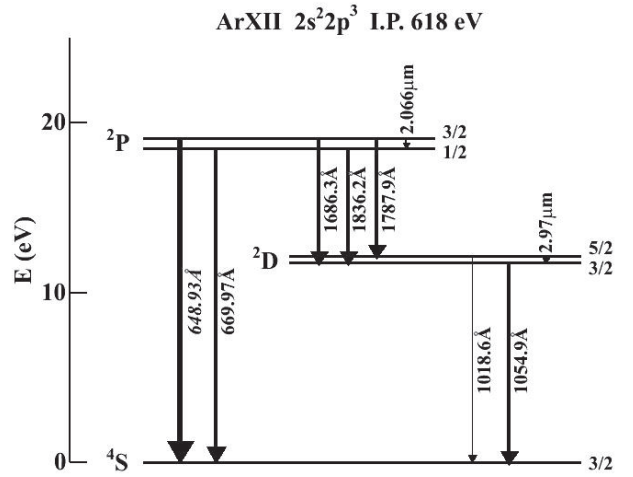


Fig. 2 Energy level diagram shows Ar XII M1 transitions in  $2s^2 2p^3$  ground configuration. Italic fonts indicate M1 transition obtained in this work. Widths of arrows show rough amplitudes of transition rates.

( $649.03 \text{ \AA}$ ) has the strongest transition rate in the diagram.

In order to confirm the identification, Doppler broadening for argon emissions was examined and compared. Figure 3 shows temporal behaviors of the ion temperature,  $T_i$ , deduced from Doppler broadening of Ar VII ( $3s3p \ ^3P_2 - 3p^2 \ ^3P_1$  :  $644.37 \text{ \AA}$ ), Ar XII M1 transition and Ar XVI Li-like resonance line ( $1s^2 2s \ ^2S_{1/2} - 1s^2 2p \ ^2P_{1/2}$  :  $389.14 \text{ \AA}$ ). The second order light was used for the Ar XVI to increase the spectral resolution. The Ar VII and Ar XII are taken from the same discharge, and the Ar XVI is taken from a similar discharge. A full width at half maximum (FWHM) of the instrumental width was checked using Ar III in low-ionized stage and determined to be 6.7 pixels. Since the observed spectral width of Ar VII is close to the instrumental width, the measured  $T_i$  has a relatively large

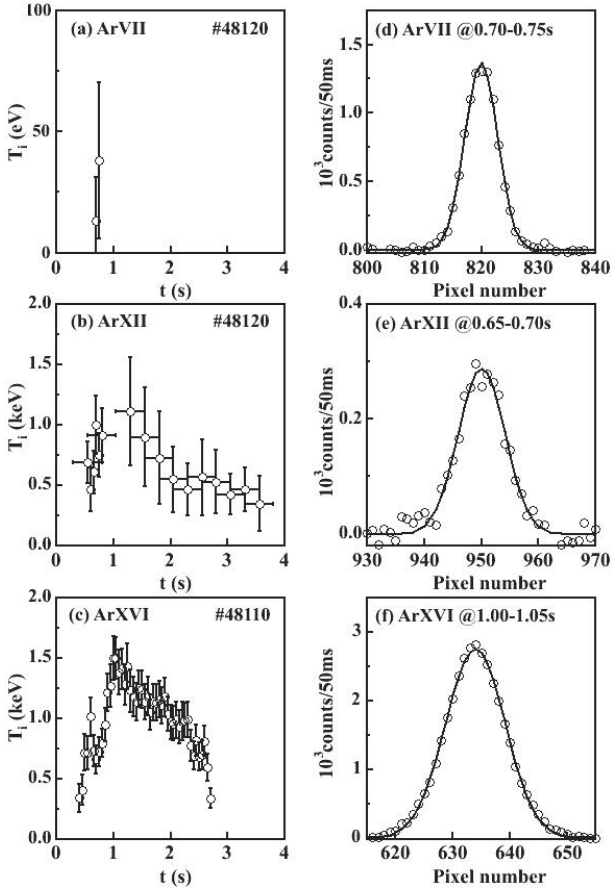


Fig. 3 Temporal behaviors of ion temperature measured from (a) Ar VII ( $3s3p^3P_2 - 3p^2\ ^3P_1$ : 644.37 Å), (b) Ar XII M1 transition ( $2s^22p^3\ ^4S_{3/2} - ^2P_{3/2}$ : 649.03 Å), (c) Ar XVI ( $1s^22s^2S_{1/2} - 1s^22p^2P_{1/2}$ : 389.14 Å). Raw data are indicated in (d), (e) and (f) taken from (a), (b) and (c), respectively, (open circles: data points, solid lines: fitting by Gaussian profile).

error bar (see Fig. 3 (a)). In contrast, the broadening of Ar XII and Ar XVI are much wider than Ar VII, as shown in Figs. 3 (d), 3 (e) and 3 (f). High Doppler temperatures are obtained for Ar XII and Ar XVI, although the  $T_i$  of Ar XVI is a little higher than that of Ar XII (see Figs. 3 (b) and 3 (c)). In argon discharges the central ion temperature reaches 8 to 10 keV. These results are very reasonable taking into account the ionization potentials (I.P.), which roughly mean the radial location;  $I.P.$  = 124 eV for Ar VII, 618 eV for Ar XII and 918 eV for Ar XVI.

A visible spectrum is shown in Fig. 4 representing four M1 transitions of Ar X ( $2s^22p^5\ ^2P_{3/2} - ^2P_{1/2}$ : 5533 Å), Ar XI ( $2s^22p^4\ ^3P_2 - 3P_1$ : 6917 Å), Ar XIV ( $2s^22p^2P_{1/2} - ^2P_{3/2}$ : 4413 Å) and Ar XV ( $2s2p\ ^3P_1 - ^3P_2$ : 5944 Å). The Ar XIV line is blended with Ar II. Those spectra were taken with an exposure time of 50 ms, whereas in the EBIT experiment an exposure time over 1 hour was necessary to get the same count rate

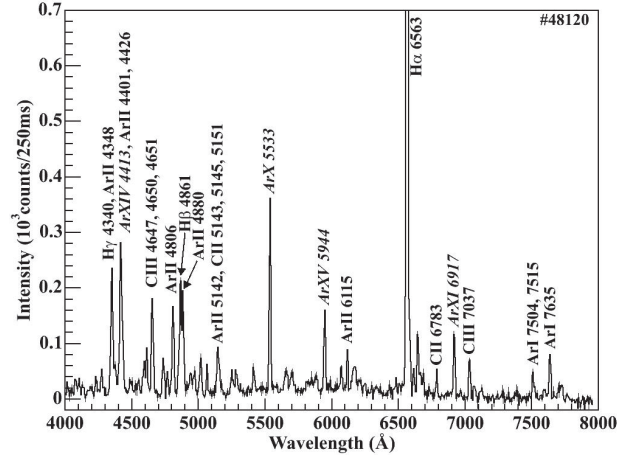


Fig. 4 Visible spectrum obtained from argon plasmas using 50 cm Czerny-Turner type spectrometer. Italic fonts indicate Ar M1 lines.

[12]. This indicates that emissions from the Ar plasmas are really brighter than from collision experiments.

Figures 5 (a)-5 (f) show temporal behaviors of Ar VII, Ar X, Ar XI, Ar XII, Ar XIV blended with Ar II and Ar XV. Only a line of Ar VII is allowed transition and other lines are the M1 transition. All the emissions rapidly increase after Ar gas puff suggesting that the indicated signals are from Ar ions. The CCD temporal resolution (50 ms) is not enough for distinction of each emission from different ionization stages at the increasing phase of intensities after gas puff was turned on. The electron temperature gradually increases and reaches 4 keV at  $t = 1.4$  s and the density keeps  $4 \times 10^{18} \text{ m}^{-3}$ . The Ar VII emission having a low ionization potential of 124 eV rapidly decreases after increase of the emission, indicating a typical behavior as an edge particle influx of Ar ions. On the contrary, behaviors of Ar XIV and Ar XV emissions having larger ionization potentials of 756 eV and 855 eV are much different from the Ar VII, especially in the decay time of the signals. These long decay times suggest a core confinement of such highly ionized Ar ions, and of course, it is confirmed that the present identification of Ar XIV and Ar XV is the unquestionable result.

The obtained M1 transitions were compared with previous works. Results are listed in Table 1 with theoretically calculated values. The wavelength of Ar XII VUV line was determined with high accuracy as presented in the table. The measured wavelength ( $649.03 \pm 0.02$  Å) obtained in the present study shows a good agreement with the theoretical value (648.93 Å). Measured wavelengths of the four visible M1 transitions (Ar X, Ar XI, Ar XIV and Ar XV) do not have a good accuracy because the spectral resolution was poor due to the usage of low-resolution gratings. The high-accuracy

Table 1 Wavelengths of Ar M1 transitions determined from the present work in comparison with previous data.

Spectra	Transition	Observed wavelengths (Å)		Calculated wavelengths (Å)	
		This work	Others	Others	Others
ArXII <sup>a</sup>	$2s^2 2p^3 \ ^4S_{3/2} - \ ^2P_{3/2}$	649.03±0.02	650 [17]	648.93	[11]
ArX <sup>b</sup>	$2s^2 2p^5 \ ^2P_{3/2} - \ ^2P_{1/2}$	5533±2	5533.265±0.002 [12]	5533.39	[11]
ArXI <sup>b</sup>	$2s^2 2p^4 \ ^3P_2 - \ ^3P_1$	6917±2	6916.878±0.012 [12]	6916 [18]	6931 [11]
ArXIV <sup>b</sup>	$2s^2 2p \ ^2P_{1/2} - \ ^2P_{3/2}$	4413±2	4412.559±0.001 [12]	4413.2 [18]	4416 [11]
ArXV <sup>b</sup>	$2s 2p \ ^3P_1 - \ ^3P_2$	5944±3	5943.880±0.005 [12]	5944	[11]

<sup>a</sup> in vacuum

<sup>b</sup> in air

measurement is possible also for the visible region. More precise measurements will be done in near future.

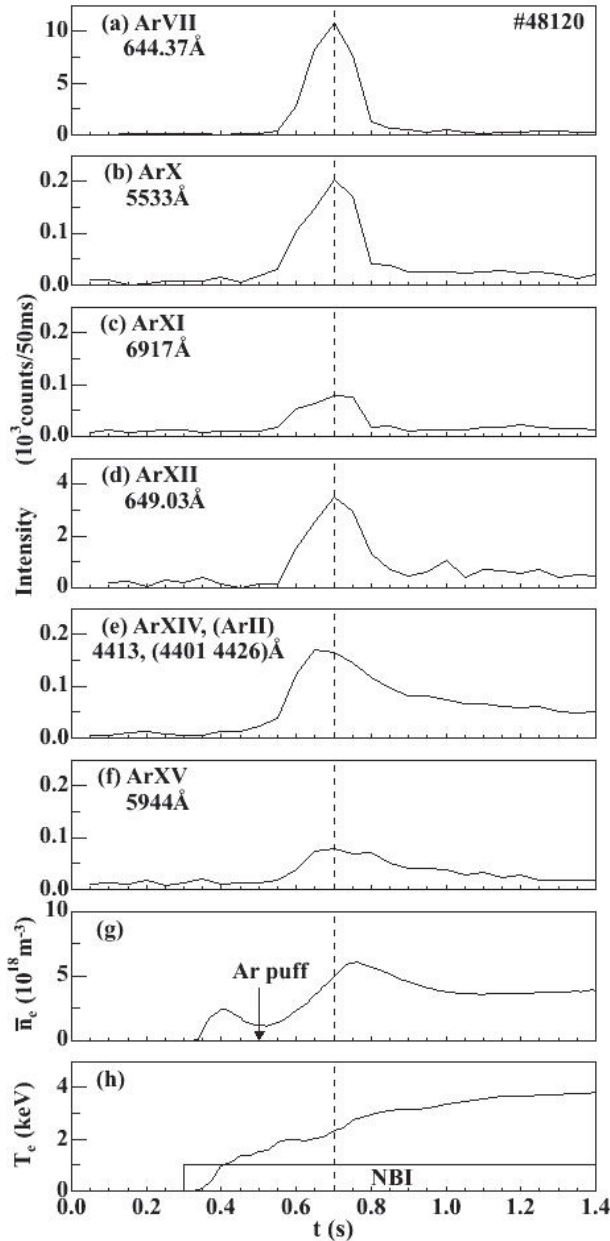


Fig. 5 Temporal behaviors of (a) Ar VII (b) Ar X (M1), (c) Ar XI (M1), (d) Ar XII (M1), (e) Ar XIV (M1) blended with Ar II, (f) Ar XV (M1), (g) line-averaged electron density and (h) central electron temperature.

## 4. Conclusions

Forbidden magnetic dipole (M1) transitions of Ar ions were found in argon discharges of LHD. One VUV lines was identified as the M1 transition of Ar XII ( $2s^2 2p^3 \ ^4S_{3/2} - \ ^2P_{3/2}$  : 649.03 Å) by analyzing the Doppler broadening. Four visible emissions of Ar X, Ar XI, Ar XIV and Ar XV were also identified as the M1 transition from the analysis of time behaviors. The emissions of the Ar M1 transitions were relatively bright, and then a regular study on the M1 transitions is possible in LHD. Further examination on the spectral structure of M1 transitions will be intentionally done in addition to the plasma diagnostics application.

## Acknowledgements

The authors would like to thank the LHD experimental group members for their effort to support the experiments in LHD.

## References

- [1] S. Suckewer and E. Hinnov, Phys. Rev. Lett. **41**, 756 (1978).
- [2] E. Hinnov *et al.*, Phys. Rev. A **25**, 2293 (1982).
- [3] K. Sato *et al.*, Phys. Rev. A **36**, 3312 (1987).
- [4] S. Suckewer *et al.*, Nucl. Fusion **19**, 1681 (1979).
- [5] K.D. Lawson *et al.*, J. Phys. B **14**, 1929 (1981).
- [6] M. Finkenthal *et al.*, J. Appl. Phys. **56**, 2012 (1984).
- [7] J.R. Roberts *et al.*, Phys. Rev. A. **35**, 2591 (1987).
- [8] E.C. Crume *et al.*, Rev. Sci. Instrum. **61**, 3147 (1990).
- [9] R. Myrnas *et al.*, Phys. Scr. **49**, 429 (1994).
- [10] A. Brown, Adv. Space Res. **6**, 977 (2003).
- [11] V. Kaufman and J. Suger, J. Phys. Chem. Ref. Data. **15**, 321 (1987).
- [12] I. Draganić *et al.*, Phys. Rev. Lett. **91**, 183001 (2003).
- [13] H. Chen *et al.*, Phys. Scr. **65**, 252 (2002).
- [14] S. Higashijima *et al.*, J. Nucl. Mater. **313-316**, 1123 (2003).
- [15] S. Morita and M. Goto, Rev. Sci. Instrum. **74**, 2375 (2003).

- [16] S. Morita and M. Goto, *Rev. Sci. Instrum.* **74**, 2036 (2003).
- [17] R.L. Kelly, *J. Phys. Chem. Ref. Data.* **16**, Suppl. 1 (1987).
- [18] B. Edlen, *Phys. Scr.* **28**, 51 (1983).